NOISE ADAPTIVE SOFT-SWITCHING MEDIAN FILTER FOR IMAGE DENOISING

*How-Lung Eng and Kai-Kuang Ma**

School of Electrical and Electronic Engineering
Block S2, Nanyang Technological University, Singapore 639798
*Email: ekkma@ntu.edu.sg

ABSTRACT

We observed that there are certain fundamental concerns commonly exist in some state-of-the-art switching-based median filters: (i) fixed thresholding for the pre-assumed noise density, (ii) the noise decision accuracy at high density impulse noise, and (iii) the filtering scheme adopted in response to pixel characteristic type identified. In this paper, we propose a novel *noise adaptive soft-switching median* (NASM) filter to effectively address the above-mentioned issues and achieve much improved filtering performance in terms of *efficiency* in removing impulse noise and *robustness* against noise density variations. Experimental results also reveal that the performance of our NASM filter is fairly close to that of ideal-switching median filter.

1. INTRODUCTION

Standard median (SM) filter was initially introduced to eliminate impulse noise with reasonably good performance achieved. Since then, it has been intensively studied (e.g., [1],[2]) and extended to promising approaches such as *weighted median* (WM)[3] and *center weighted median* (CWM)[4] filters. Applying any median filtering to the entire image would inevitably remove some detailed information of the image. Ideally, median filtering should be only applied to corrupted pixels while leaving those uncorrupted ones intact. Therefore, a detection process for separating the uncorrupted pixels from the corrupted ones, prior to applying any nonlinear filtering, is highly desirable. To achieve this objective, Sun and Neuvo [5] and Florencio and Schafer [6] have proposed their *switching-based* median filtering methodologies by applying—"no-filtering" to true pixels and SM filter to impulse noise. However, we observe certain fundamental concerns inherited in these schemes as follows.

Firstly, the above-mentioned algorithms exploit a fixed decision-making threshold which is obtained at a pre-assumed noise density level. When applying the same algorithms to noisy images under different noise density levels, large mismatch will cause substantial degradation of the filtering performance. Secondly, at high density impulse noise, those noise detection processes often lead to incorrect discrimination between pixel and noise. Thirdly, when misclassification happens, more sophisticated filtering scheme—also serving as a compensation process, is desirable to have for effective removing of corrupted pixels while preserving the image details. In this paper, a novel *noise adaptive soft-switching median* (NASM) filtering method is proposed to address these concerns with architecture as shown in Figure 1.

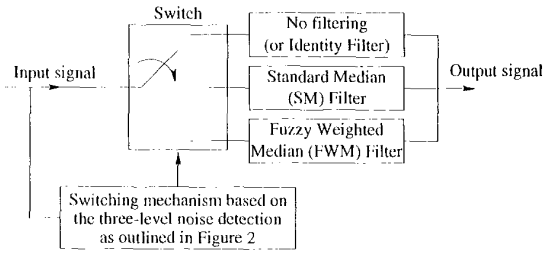

Figure 1: Architecture of our proposed *noise adaptive soft-switching median* (NASM) filter.

Our proposed NASM filter contains a switching mechanism steered by a three-level noise detection process for determining each pixel's characteristic type, followed by invoking proper filtering action, as outlined in Figure 2. In our proposed noise detection scheme, global or local pixel statistics have been utilized in the respective decision-making level. Action "no filtering" will be invoked if the considered pixel is identified as uncorrupted. Otherwise, SM or our proposed *fuzzy weighted median* (FWM) filtering would be carried out to remove identified impulse noise (e.g., either isolated or belonging to a noise blotch) or preserve edge pixels, respectively. The proposed FWM filter was designed to maximize impulse noise attenuation while preserving image details, when mis-classification happens.

2. THREE-LEVEL NOISE DETECTION SCHEME

For each image pixel, a three-level noise detection process is performed to identify the pixel as one of the four characteristic types: (i) *uncorrupted pixel*, (ii) *isolated impulse noise*, (iii) *non-isolated impulse noise*, and (iv) *edge pixel*, as indicated at the decision tree nodes in Figure 2.

2.1. Level 1: Detection of uncorrupted pixel

The identification of "*uncorrupted*" pixel in this level is performed by utilizing the *global* statistics of the pixel intensities. Impulse noise corrupt the image pixels to either very

0-7803-6293-4/00/$10.00 ©2000 IEEE.

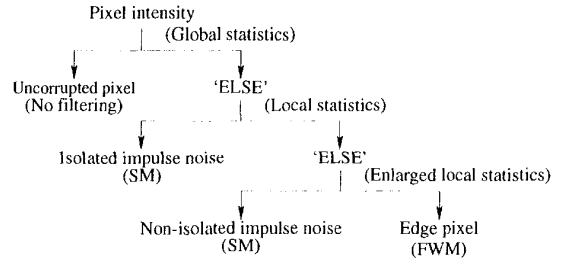

Figure 2: Hierarchical identification of pixel's characteristic based on a three-level noise detection process. There are four pixel characteristic types corresponding to the four nodes, respectively.

high or very low value. By analyzing the gray-level difference between the noisy image and an estimation of the original (i.e., uncorrupted) image pixel-wise, it is expected that uncorrupted pixels should yield much smaller difference values as compared with that of the corrupted ones.

The estimated original image is obtained by passing the noisy image through a SM filter with window size of $W_{D1} \times W_{D1}$. For that, the processing steps will be iterated twice to (i) estimate the noise density level p in the first iteration such that approximate window size could be determined based on Table 1, and (ii) repeat the same processing steps in the second iteration using the window size determined in the first iteration. To start the first iteration, fixed window size 7×7 is applied, and the noise density level p could be estimated by simply calculating the percentage of *uncorrupted pixels* identified.

To achieve better identification of uncorrupted pixel, the estimated original image is decomposed into non-overlapping homogeneous blocks based on conventional quadtree decomposition technique. For each homogeneous block, the corresponding pixel-wise difference Δ_i between the noisy image and the estimated original image is computed independently. It is observed that *uncorrupted* pixels will contribute to the distribution around the center as they tend to yield much smaller Δ_i values, individually. Whereas, *corrupted* pixels and/or *edge* pixels tend to correspond to both tails of the distribution.

Two optimal partition parameters, p_l and p_u, are derived to partition the distribution of Δ_i into three non-overlapping ranges such that all the pixels with Δ_i falling on the center range $[p_l\ p_u]$ are considered as being "uncorrupted".

Consider the positive part of the distribution; i.e., $\Delta_i \geq 0$. Denote $x_o, \ldots, x_m$ as the bin values of the error histogram of Δ_i and $x_0 \leq x_1 \leq \ldots \leq x_m$. Quantity n_i (for $i = 0, \ldots, m$) indicates the number of elements in each bin, respectively. Parameter p_u is derived to be,

$$p_u = \frac{2}{\sum_{i=0}^{m} n_i}\Big[\sum_{i=0}^{m/2-1} n_i\,(x_i - \frac{x_0}{2}) + \sum_{i=m/2}^{m} n_i\,(x_i - \frac{x_m}{2})\Big] \ . \quad (1)$$

Similar analysis is repeated for the negative part of the distribution; i.e., $\Delta_i < 0$. Let bin values $x_{-m} \leq x_{-m+1} \leq \ldots \leq x_{-1}$, and n_i represents the number of elements in each bin, respectively. Parameter p_l is obtained as

Noise density (p%)	Suggested $W_{D1} \times W_{D1}$
$0 < p \leq 15$	3×3
$15 < p \leq 30$	5×5
$30 < p \leq 45$	7×7
$45 < p \leq 60$	9×9
$60 < p \leq 70$	11×11

Table 1: Suggested window dimension of $W_{D1} \times W_{D1}$ for the noise density level p being estimated.

$$p_l = \frac{2}{\sum_{i=-m}^{-1} n_i}\Big[\sum_{i=-m}^{-m/2-1} n_i\,(x_i - \frac{x_{-m}}{2}) + \sum_{i=-m/2}^{-1} n_i\,(x_i - \frac{x_{-1}}{2})\Big] \ . \quad (2)$$

2.2. Level 2: Detection of isolated impulse noise

Local statistics based on a $W_{D2} \times W_{D2}$ decision window, where odd integer W_{D2} satisfies $3 \leq W_{D2} \leq W_{D1}$, is utilized to identify *isolated impulse noise*. Fuzzy set approach is proposed, and only those uncorrupted pixels (identified in Level 1) within the window are considered on computing their membership values with respect to the center pixel.

The membership value of *uncorrupted* pixels within $W_{D2} \times W_{D2}$ is defined as:

$$\mu_{s,t} = \left(\sum_i \sum_j \frac{d_{s,t}}{d_{i,j}}\right)^{-1} , \quad (3)$$

for $-(W_{D2}-1)/2 \leq s,t \leq (W_{D2}-1)/2$, and coordinate (i,j) corresponds to all the *uncorrupted pixels* within the window. Parameters $d_{s,t}$ and $d_{i,j}$ are the differentials of the center pixel's intensity with respect to that of its neighboring uncorrupted pixels, individually. Starting with $W_{D2} = 3$, the decision window iteratively extends the window's boundaries outward symmetrically by one pixel in all directions in each iteration, if the number of *uncorrupted pixels* is less than $(W_{D2} \times W_{D2})/2$ until $W_{D2} = W_{D1}$.

The above-mentioned approach essentially transforms the "*pixel map*" into the "*membership map*". By adopting the same binarization method used in *absolute moment block truncation coding* (AMBTC) [7], the mean of membership map $\mu_{s,t}$ is used to divide the map into two groups—higher-value group representing "closely correlated pixels" and lower-value group indicating "less correlated pixels". The average of each group's membership values $\mu_{s,t}$ is computed and denoted as μ_h and μ_l, respectively.

Membership value of 0.75 is chosen as the confidence limit to assign the considered pixel to the higher-value group. Thus, the decision rules for detecting *isolated impulse noise* are summarized as follows:

Condition 1: If $\mu_l/\mu_h > 1/3$, the pixel is considered as an *isolated impulse noise*. SM filtering would be carried out to filter that impulse noise.

Condition 2: If $\mu_l/\mu_h \leq 1/3$, the pixel is considered as belonging to a small correlated pixel block, which could be either a noise block or a cluster of edge pixels. Thus, further discrimination is required and described as follows.

2.3. Level 3: Discrimination between non-isolated impulse noise and edge pixel

Both *non-isolated impulse noise* and *edge pixel* are high frequency signals in essence; thus, they are most difficult to be discriminated. To further extend the $W_{D2} \times W_{D2}$ window obtained in the second-level detection in the direction for including more correlated pixels will increase the decision accuracy, since the percentage of correlated pixels in the enlarged window will increase for *edge pixel* but decrease for *non-isolated impulse noise.*

To do so, the algorithm checks if any window boundary of the $W_{D2} \times W_{D2}$ decision window contains at least one "closely correlated pixel" (corresponding to those pixels exploited on computing parameter μ_h as described in Level 2), and the corresponding boundary will then be subsequently extended outward by one pixel. If the total number of "closely correlated pixels" is greater than threshold S_{in}, the considered pixel is viewed as *edge pixel*; otherwise, is treated as *non-isolated impulse noise.* Threshold S_{in} has been conservatively defined to be half to the total number of uncorrupted pixels within the enlarged window.

3. FILTERING SCHEME

In the filtering scheme, action "no filtering" is applied to those uncorrupted pixels identified. Besides, SM filter with window size of $W_F \times W_F$ is exploited, and the output pixel Y_{ij} is given by

$$Y_{ij} = \text{median}\Big\{ X_{i-s,j-t} \mid (s,t) \in W \Big\} \tag{4}$$

where $W = \big\{(s,t) \mid -(W_F-1)/2 \le s,t \le (W_F-1)/2\big\}$, and only *uncorrupted* pixels are considered for the ranking process. Filtering window $W_F \times W_F$ is obtained in the same way as decision window $W_{D2} \times W_{D2}$; thus, $3 \le W_F \le W_{D1}$.

Owing to inevitable mis-classification of noise blotches as edge pixels, a sophisticated *fuzzy weighted median* (FWM) filter is proposed to strike a balance between preserving edge pixels and removing those noise blotches identified. Fuzzy membership function $\mu_{s,t}$ obtained earlier is re-used to determine all the weights of uncorrupted pixels within that $W_F \times W_F$ window, except for the center pixel, as follows.

By minimizing the output data variance σ^2_{wm} as defined in Equation (3) of [8], we obtain

$$\mu_c = \frac{\sum_s \sum_t \mu^2_{s,t}}{\sum_s \sum_t \mu_{s,t}}, \quad \text{for } (s,t) \neq (0,0). \tag{5}$$

The weighting factors of the *uncorrupted pixels* within the $W_F \times W_F$ filtering window are

$$\omega_{s,t} = \begin{cases} \frac{\mu_{s,t}}{X}, & \text{for } (s,t) \neq (0,0); \\ \frac{\mu_c}{X}, & \text{if } s = t = 0, \end{cases} \tag{6}$$

where $X = \sum \mu_{s,t} + \mu_c$, and μ_c/X is the weighting factor assigned to the center pixel. Therefore, the filtered output of pixel $X_{i,j}$ is

$$Y_{i,j} = \text{median}\Big\{ \omega_{i-s,j-t} \diamond X_{i-s,j-t} | (s,t) \in W \Big\} \tag{7}$$

where symbol $\diamond$ denotes the duplication operation.

4. SIMULATION RESULTS

4.1. Noise detection performance

To appreciate the performance contributed from each decision level in Figure 2, parameters *correct detection* ξ and *mis-classification* ζ are established and defined as follows,

$$\xi = \frac{\text{corrupted (uncorrupted) pixels detected}}{\text{total corrupted (uncorrupted) pixels in the image}} \tag{8}$$

$$\zeta = \frac{\text{corrupted (uncorrupted) pixels misclassified}}{\text{total corrupted (uncorrupted) pixels in the image}}. \tag{9}$$

These two parameters are used to measure the percentage of corrupted or uncorrupted pixels of the noisy image being correctly or incorrectly classified at each decision node, respectively. From Table 2, it shows that the detection of *uncorrupted* pixels achieves over 97% of correct detection, indicating that the first-level noise detection successfully plays the dominant role in preserving image details. Furthermore, the correct classification of *isolated impulse noise* is over 99% for noise density level $p \le 30\%$. At very high noise density level, $p \ge 50\%$, impulse noise tend to form noise blotches rather than isolated ones; thus, they are much harder to be detected. With the third-level noise detection, the presence of noise blotches has been re-detected and classified as *non-isolated impulse noise.*

4.2. Overall filtering performance

The *peak signal-to-noise ratio* (PSNR) performance of the proposed NASM was compared with that of the 3×3 SM filter, 3×3 CWM [4] filter (with center weight $\omega_c = 3$), Florencio and Schafer's switching scheme [6], Sun and Neuvo's switching scheme-I [5] and our proposed *ideal-switching* filtering. We introduce ideal-switching filter here such that it can be served as the theoretical upper bound (in dB) for all the switching-based median filters, in order to gauge their filtering performance and potential. The ideal-switching filter is only achievable through simulation where the position of each impulse noise injected has been exactly recorded for the follow-up median filtering process.

The extrapolated PSNR curves resulted from using various median filters at different noise densities ranging from 10% to 70% for "Lena" image are shown in Figure 3 . The proposed NASM filter significantly outperforms other filtering schemes by having a much slow decaying PSNR curve and is much closer to that of the ideal-switching filter. This shows the robustness of our NASM filter against wide variation of impulse noise. Figure 4 shows a subjective visual comparison of the denoising performances of various methods when the impulse noise density is imposed at $p = 60\%$.

5. CONCLUSION

In this paper, a novel median filtering scheme, named *noise adaptive soft-switching median* (NASM) filter, is introduced. The proposed NASM filter has addressed three main concerns commonly found in certain state-of-the-art *switching-based* median filters: (i) adaptiveness and sensitivity of decision-making threshold, (ii) accuracy of the noise-detection

Noise density (p%)	Uncorrupted pixel		Isolated impulse noise	
	ξ (%)	ζ (%)	ξ (%)	ζ (%)
10	97.321	0.110	99.633	1.066
30	99.358	0.127	99.312	0.172
50	99.436	0.420	75.912	0.092
70	98.608	0.615	20.873	0.321
Noise density (p%)	Non-isolated impulse noise		Edge pixel	
	ξ (%)	ζ (%)	ξ (%)	ζ (%)
10	0.087	0.281	1.333	0.170
30	0.309	0.106	0.363	0.252
50	21.876	0.159	0.312	1.792
70	72.783	0.640	0.431	5.728

Table 2: *Correct detection* ξ and *mis-classification* ζ yielded at each terminal node in Figure 2 for "Lena" image.

process, especially at high noise density, and (iii) suitability of the median filtering scheme exploited.

In our NASM filtering architecture, the switching mechanism is steered by a three-level noise detection process to classify each pixel into one of the four pixel categories. Experimental results reveal that our NASM filtering algorithm significantly outperforms other state-of-the-art *switching-based* median filters by having much higher PSNR values and more stable performance across a wide range of noise densities, varying from 10% to 70%.

Furthermore, the architecture of NASM filter is generic to be used for one-dimensional and multi-dimensional signals. We have applied our NASM filter for smoothing out irregular macroblock motion vectors extracted directly from MPEG bitstreams for the application of video indexing and retrieval [9].

6. REFERENCES

[1] I. Pitas and A. Venetsanopou, *Nonlinear digital filters: principles and applications*. Kluwer Academic Publishers, 1990.

[2] J. Astola and P. Kuosmanen, *Fundamentals of nonlinear digital filtering*. CRC Press, 1997.

[3] D. Brownrigg, "The weighted median filter," *Comm. Assoc. Computer*, pp. 807-818, March 1984.

[4] S.-J. Ko and Lee, "Center weighted median filters and their applications to image enchancement," *IEEE Trans. on Circuits and Systems*, vol. 15, no. 9, pp. 984-993, 1991.

[5] T. Sun and Y. Neuvo, "Detail-preserving median based filters in image processing," *Pattern Recognition Letters*, vol. 15, pp. 341-347, 1994.

[6] D. Florencio and R. Schafer, "Decision-based median filter using local signal statistics ," *Proc. of the SPIE Intl. Symposium on Visual Comm. and Image Processing*, Sept. 1994, Chicago, Illinois, USA.

[7] K.-K. Ma, "Put absolute moment block truncation coding in perspective," *IEEE Trans. on Comm.*, pp. 284-286, March 1997.

[8] R. Yang, M. Gabbouj and Y. Neuvo, "An efficient design method for optimal weighted median filtering," *IEEE Intl. Symposium on Circuits and Systems (ISCAS)*, pp. 633-636, 1994.

[9] H.-L. Eng and K.-K. Ma, "Motion trajectory extraction based on macroblock motion vectors for video indexing," *IEEE Intl. Conference on Image Processing*, 23-25 Oct. 1999, Kobe, Japan.

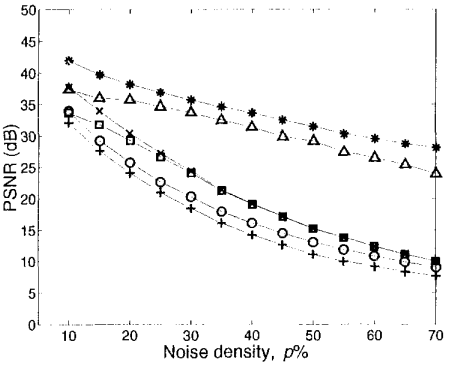

Figure 3: Performance comparison using various median filtering techniques with noise density varying from 10% to 70% for "Lena" image. (Legends: '□' for SM; 'o' for CWM; '+' for Florencio and Schafer's Switching Scheme; '×' for Sun and Neuvo's Switching Scheme-I; '△' for our NASM; '*' for Ideal-Switching)

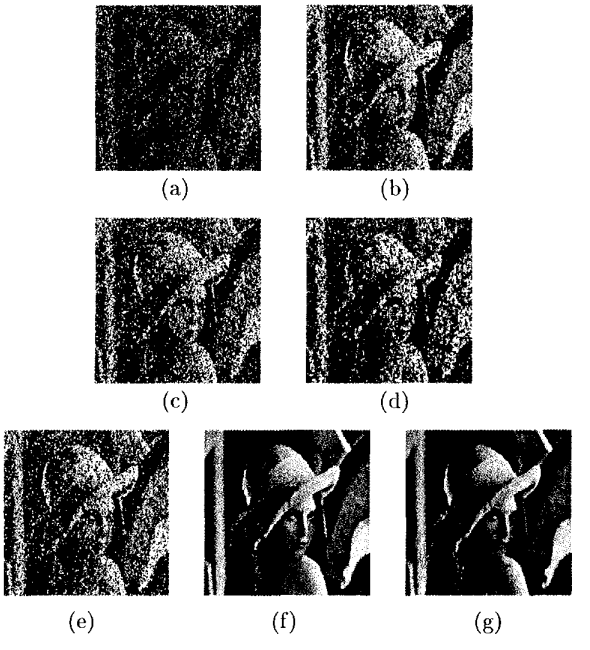

Figure 4: (a) Corrupted "*Lena*" image with impulse noise density, p=60%. Filtered images using: (b) SM; (c) CWM; (d) Florencio and Schafer's Switching Scheme; (e) Sun and Neuvo's Switching Scheme-I; (f) our NASM; and (g) Ideal-switching filtering. Note that the proposed NASM filter achieves almost unnoticeable difference as compared with the Ideal-switching filter.